EXPERIMENTAL INVESTIGATIONS OF PRECAST BRIDGE COLUMNS

W. Xu[(1)], B. Ma[(2)], X. Wang[(3)], J. Li[(4)]

[(1)] *Ph.D. Candidate, School of Civil Engineering, Tongji University, China, xuwenjing@tongji.edu.cn*
[(2)] *Professor Senior Engineer, Shanghai Municipal Engineering Design Institute (Group) Co. Ltd, China, mabiao@smedi.com*
[(3)] *Ph.D. Candidate, School of Civil Engineering, Tongji University, China, 1610178@tongji.edu.cn*
[(4)] *Professor, School of Civil Engineering, Tongji University, China, lijianzh@tongji.edu.cn*

Abstract

Accelerated bridge construction (ABC) utilizes new techniques, advanced planning, and novel detailing to expedite constructions, which has attracted substantial attention all over the world. Accelerated bridge construction offers many benefits, such as lower traffic impact, shorter onsite construction time and higher quality structural members compared with the conventional construction techniques. Precast systems and members are the important components of ABC. Several prefabrication connections have been common in low and moderate seismic regions, however, the implementation of precast columns in high seismic zones has been limited because of a lack of performance data pertaining to their connections. Mechanical bar splice, such as grouted steel sleeves, as one of the precast column connections has been emphasized in precast bridge columns. These connections can shorten the splice length and reduce bar congestion in the connection. Furthermore, besides the mechanical bar splices, in recent years, importance and necessity of using high strength materials is recognized in precast systems. Therefore, in this paper, seismic performance of two large-scaled prefabricated columns were experimentally investigated through the quasi-static testing, one precast bridge column with grouted sleeves connections and the other one with a new column-to-footing connection incorporating an ultra-high performance concrete (UHPC). The damage process, the drift capacity, the resilience behavior and the hysteresis energy response of the two large-scaled prefabricated columns were described and discussed. Test results showed that the performance of the two columns with different connections are able to meet seismic demand. The failure mode of the precast column with grouted sleeves connections was bar fractured. This occurred because grouted sleeves are very stiff and when the grouted sleeves length is large, the plastic hinge area is mainly located at the joint of the column bottom, so that lead to rebar strain concentrations adjacent to the end of the sleeves. As for the precast column connected with ultra-high performance concrete (UHPC), based on the observations of test results, the failure mode was the conventional core concrete crushed above the connection region, and no damage such as cover concrete spalling, bar pullout, core concrete failure of the connected region was observed in the column-to-footing connection with ultra-high performance concrete (UHPC).

Keywords: precast bridge columns; grouted sleeves; UHPC; seismic performance; cyclic test

1. Introduction

Recently, many successful applications of accelerated bridge construction (ABC) technique have been realized in practical bridge projects. ABC provides many advantages such as shorter onsite construction time, potentially lower cost, less traffic impact and improved construction quality and safety [1, 2]. It has become a trend for the next generation of bridge structures. Prefabricated bridge substructures as an essential part of ABC technique has received more attention in recent studies. The connections of precast bridge piers must not only be easy to construct, but also must be robust enough to reduce damage under seismic loading.

Several prefabricated connection types of precast bridge piers have been tested for seismic loading and deployed in seismic regions of the United States [3]. These connections could be classified into bar coupler connections, grouted duct connections, pocket connections, member socket connections and hybrid connections according to force transfer mechanisms [4]. Grouted steel sleeves as one of the bar coupler type connection is most commonly used in bridges. These connections can shorten the splice length and reduce bar congestion in the connection, but the experimental results showed that the precast pier with grouted steel sleeves had a lower displacement ductility capacity than that of the cast-in-place (CIP) pier [5].

Besides these abovementioned connection types, the employment of advanced construction materials is alternative access to ensure firm connection between precast elements. Recently, with the advent of advanced materials and technology, ultrahigh performance concrete (UHPC) has come into our sight. As a class of cementitous composite material, UHPC exhibits compressive strength above 150 MPa with improved durability and enhanced stability over conventional concrete [6]. Additionally, of particular interest to researchers, UHPC can exhibit excellent anchoring properties which could shorten the bar embedment length. Tazarv et al. [7] designed 14 pullout specimens to study the bond behavior of UHPC filled duct connections under tensile loading and the test results indicated that UHPC had exceptional bond capacity which could significantly reduce the bar embedment length.

These excellent properties of UHPC make it a superior candidate for precast connections. The Federal Highway Administration [8] found that using UHPC as a closure pour joint fill could allow for better joint interface bonding and long-term durability. Tazarv and Saiidi [9] put forward a new column-to-footing connection incorporation an UHPC filled duct. A half-scale precast concrete circular column was tested and the results indicated this type of column-to-footing connection was emulative of a conventional monolithic connection. Furthermore, the tests on the seismic performance of using UHPC at the plastic hinge region of the column were conducted by Ichikawa et al [10], and it was found that using UHPC at the plastic hinge region could minimize damage under seismic loading.

In this paper, seismic performance of two large-scaled prefabricated columns with different connection types were experimentally investigated through the quasi-static testing. One precast bridge column used grouted sleeves connections and the other one used a new column-to-footing connection incorporating UHPC. The damage process, drift capacity, resilience behavior and hysteresis energy response of the two large-scaled precast columns were described and discussed.

2. Design of test specimens

Two large scaled precast bridge column specimens were designed for testing under lateral cyclic loadings. One of the specimen was referred to as “PGS”, an acronym for precast column with grouted sleeves, and the other one was referred to as “PUC”, and acronym for precast column with UHPC-filled connection.

2.1 PGS specimen description

Fig.1 shows the tested configuration of the PGS specimen. The specimen shear height was 4210 mm and the corresponding shear span ratio was 7. The column was a standard rectangle cross-section of 600 × 600 mm. The cap beam and the footing were designed as rectangle elements of 900 by 900 by 3000 mm and 2400 by 2400 by 600 mm (width by length by height), respectively. For the column, four Φ40 mm bars were used to be longitudinal bars and corresponding longitudinal steel ratios was 1.4%, as shown in Section A-A, and Φ

12 mm bars were employed to be stirrups with vertical spacing was 100 mm. Four grouted sleeves with 800 mm length were embedded in the plastic hinge area of the column and the reinforcement details of the grouted sleeves region as shown in Section B-B.

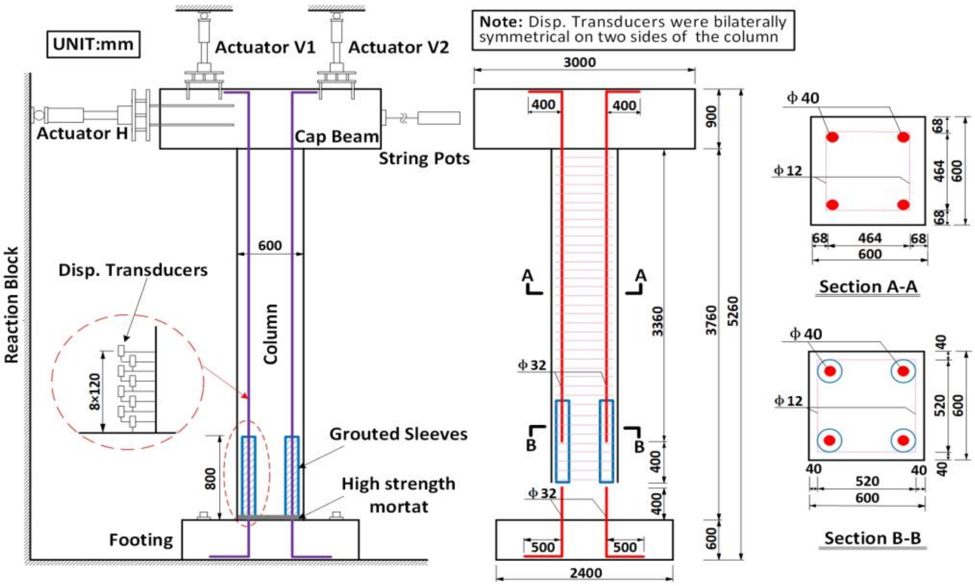

Fig. 1 – Details of the PGS specimen

The process of PGS specimen assemblage is shown in Fig.2. Firstly, prefabricated the column with grouted sleeves at the bottom of the column (Fig. 2(a)) and casted the footing with extended bars (Fig. 2(b)). Then with the help of the crane, the column segment was placed in the scheduled location of the footing top surface, like Fig .2 (c) and (d). When assembled completely, grouted the sleeves to achieve the connection between the column and the footing (Fig. 2(e)). Eventually, Fig. 2(f) shows the finished PGS specimen before loading.

Fig. 2 – Construction sequence of the PGS specimen

2.2 PUC specimen description

The key dimensions and reinforcement of the PUC specimen are shown in Fig.3. The specimen was assembled with three precast parts: a cap beam, an integrated column and a rigid footing. The column height from top of the footing to the loading point was 4210 mm and it was mentioned that both end regions of the column were designed a hollow cage for grouting UHPC. Therefore, the solid section with 600 × 600 mm of column mid-portion (Section A-A) was enlarged to the hollow one with the length, width and the height of 800, 800 and 440 mm, respectively, like Sections B-B and C-C in Fig.3. The cap beam and the footing were designed as capability protection components. The mid-portion of column was reinforced longitudinally with Φ32 mm bars and transversely with Φ10 mm stirrups, resulting in longitudinal steel ratios of 1.8%. The Φ 32 mm longitudinal bars of the cap beam and footing were both extended 400 mm at the surface to be inserted into the hollow cage of the column respectively. The essential reinforcement details of the column enlarged portion were depicted in Fig.3.

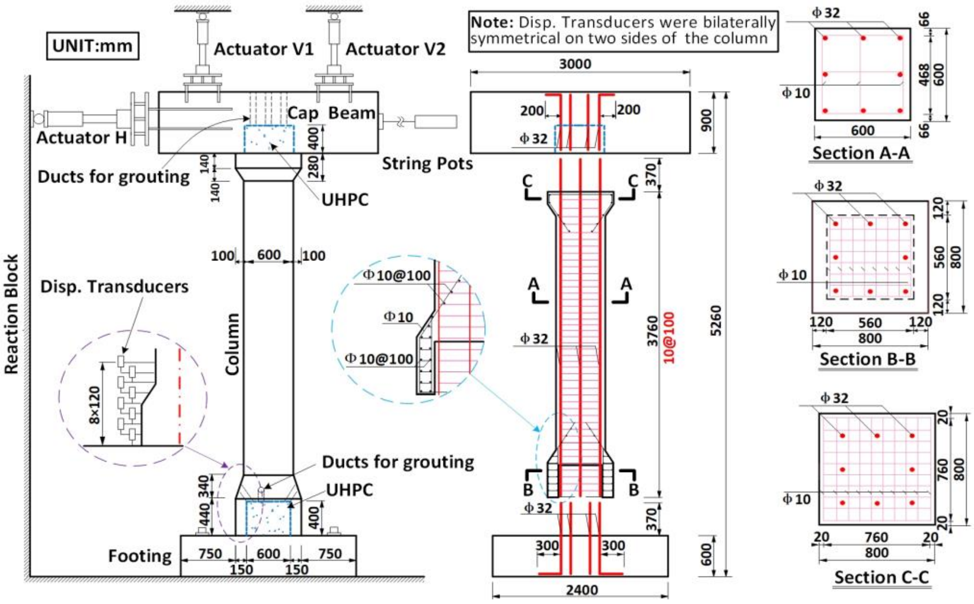

Fig. 3 – Details of the PUC specimen

Fig. 4 shows the process of PUC specimen construction. The construction stages of the PUC specimen were first casting the footing and cap beam with extended steel bars on the surface (Fig. 4(a)). Next, casted the column with hollow cages and extended longitudinal bars both at the top and bottom of the column as shown in Fig. 4(b). Then erected the column segment of the footing and cap beam surface (Fig. 4(c)), and filled the cage with UHPC through the reserved 80 mm diameter duct (Fig. 4(d)). The finished PUC specimen was shown in Fig. 4(e).

Fig. 4 – Construction sequence of the PUC specimen

3. Test setup and loading protocol

A horizontally aligned servo-controlled hydraulic actuator (Actuator H), whose one end fixed to the reaction wall as shown in Fig.1 and Fig.3, was used in the test to apply lateral loads to specimens. The maximum load capacity and travel distance of this actuator are 1000 kN and ±500 mm, respectively. In addition, two vertical actuators (Actuators V1 and V2) were symmetrically implemented on top surface of the cap beam to supply a constant axial load of 906 kN for both the PGS specimen and the PUC specimen. The vertical actuators can laterally slip with the movement of the cap beam during the testing process to guarantee the applied axial load in the vertical line. Both the PGS specimen and the PUC specimen were subjected to cyclic force-control levels firstly, and after the longitudinal rebar yielding, the loading model was changed to displacement-control loading. Three full cycles were applied at each load level to determine the strength and stiffness degradation of the specimens.

Both specimens tested in this paper were heavily instrumented with displacement transducers, string potentiometers, strain gauges and load cells. The detailed arrangement of displacement transducers and string potentiometers for PGS specimen and PUC specimen were shown in Fig.1 and Fig. 3 respectively. Sixteen displacement transducers were used at eight critical locations on the lower part of the column to measure the plastic hinge curvature variations. One string pot was installed on the cap beam to measure the lateral displacement of the column. Meanwhile, lots of strain gauges were installed at the key sections of the columns to measure longitudinal and transverse reinforcement strains.

4. Experimental results

4.1 Observed damage

The overall damage of the PGS specimen at different loading conditions is shown in Fig.5. The first crack appeared in the middle of the sleeves section (400 mm from the column bottom) and above the sleeves section (1000 mm from the column bottom) in the initial stage of force-control loading, as shown in Fig. 5(a). At the end of force-control loading, the longitudinal bars yielded and the number of cracks increased as shown in Fig. 5(b). After that, loading method changed to displacement-control loading. When the displacement loading reached to 2.8% drift, the cover concrete spalled at the corner of the column (Fig. 5(c)) and the mortar at the bottom of the column crushed where could see the bottom of the sleeves through the damage, like Fig. 5(d).

When the displacement loading reached to 3.6% drift ratio, the longitudinal bars fractured at the joint of the column and footing, which could be seen in Fig. 5(e) and Fig. 5(f). In the meantime, the lateral force dropped to 80% of the lateral load-resisting capacity and the specimen reached the ultimate failure state. It can be seen from the test phenomenon that the damage was concentrated at the joint of the column and footing, and the concrete in the plastic hinge region was almost no damage. This was due to the large rigidity of the sleeves which formed a rigid region in the connection portion so as to resulting in curvature increasing and rebar strain concentrations adjacent to the end of the sleeves.

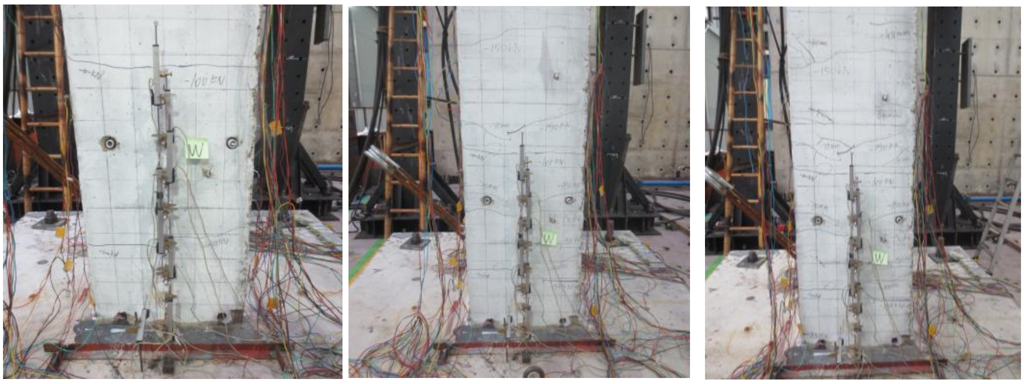

(a) (b) (c)

(d) (e) (f)

Fig. 5 – Damage progression of the PGS specimen

Fig.6 shows the PUC specimen damage at different loading stages. During loading, the crack appeared first in the ordinary concrete region of the column, like Fig.6 (a). With the loading increasing, cracks developed significantly, as shown in Fig. 6(b). After the longitudinal bars yielding, the loading mechanism changed from force-control loading to displacement-control loading, and at the same time, the crack spread to the enlarged region of the column, like Fig. 6(c). When the displacement loading reached to 2.5% drift ratio, the specimen reached the peak load and the cover concrete above the enlarged region spalled, as shown in Fig. 6(d), after that, with the drift ratio increasing, the lateral force of the specimen decreased.

When the displacement loading reached to 4.5% drift ratio, concrete spalled within 500 mm from the top of the enlarged region of column was visibly observed, seen in Fig. 6(e). Since the spalled regions significantly extend, the crushing of the core concrete was unavoidable. When the drift ratio was 5%, the exposure of longitudinal bars and stirrups could be clearly seen as shown in Fig. 6(f), and the lateral force dropped to 80% of the peak load at the same time. However, there was no damage in the connection region until the loading finished (Fig. 6(f)).

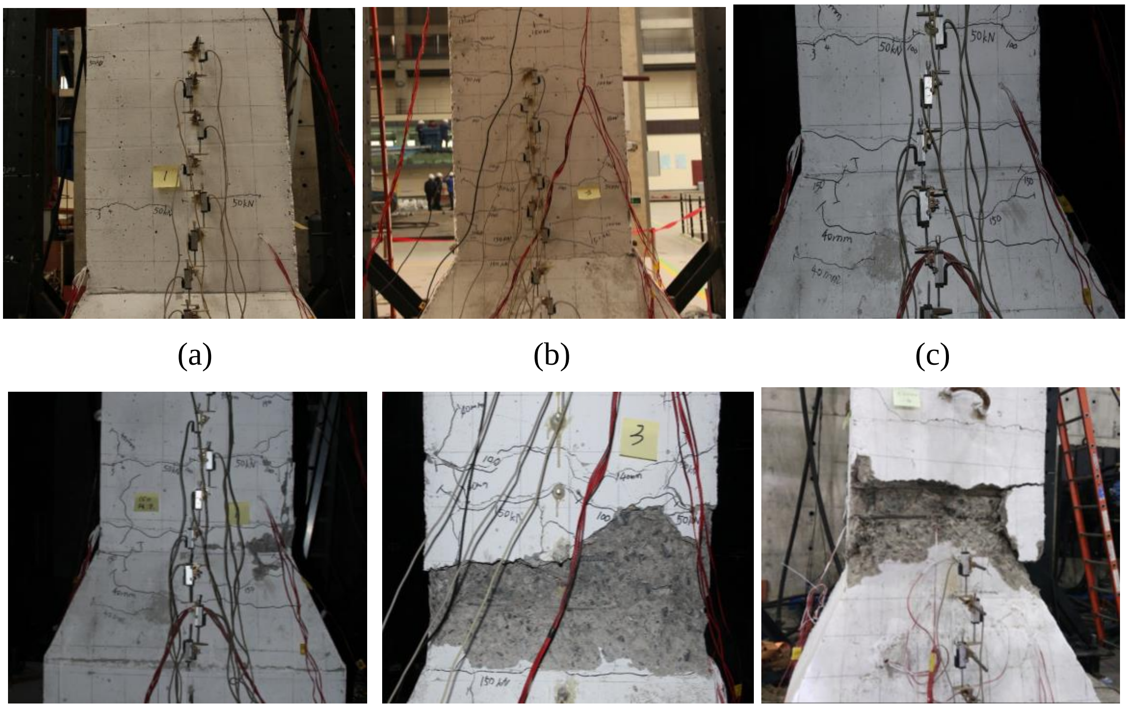

(a) (b) (c)

(d) (e) (f)

Fig. 6 – Damage progression of the PUC specimen

4.2 Force-displacement relationship

The measured lateral force-drift hysteretic curves for the PGS specimen and the PUC specimen are shown in Fig.7. The PGS specimen exhibited minor strength degradation at the beginning of the load. As the concrete cracks appearing and the longitudinal bars yielding, the hysteresis loop became wider, and at the later stage of loading, the hysteresis loop gradually became a flat quadrilateral and the residual displacement increased obviously. There was a sharp decline in the hysteresis curve when the displacement loading reached to 3.6% drift ratio, as shown by the red line in the Fig. 7(a), which represented the longitudinal bars fractured and the specimen destroyed. The PUC specimen exhibited stable hysteretic loops with minor strength degradation at the initial stage and later, the strength had been slowly decreasing until the core concrete crushed, like Fig. 7(b). The ultimate drift of the PUC specimen was nearly 5%.

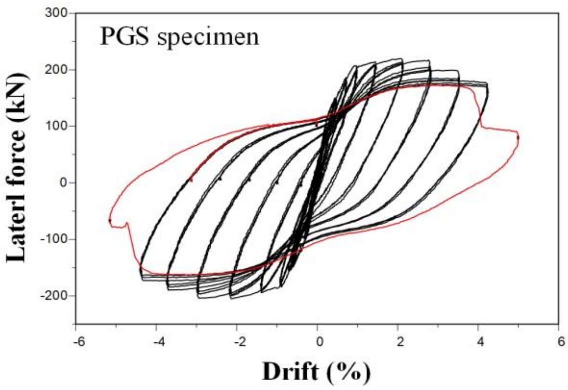

(a) PGS specimen

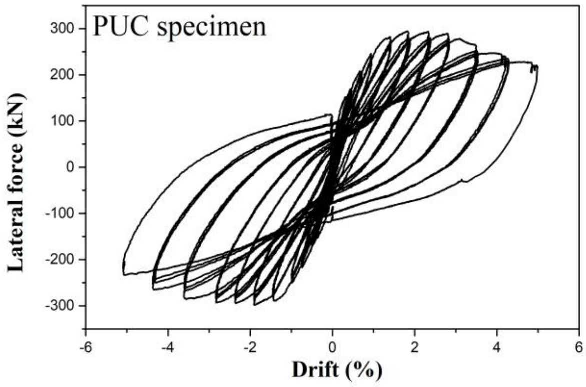

(b) PUC specimen

Fig. 7 – Force-drift hysteretic responses

The average push and pull force-drift envelope of the PGS specimen and the PUC specimen are shown in Fig.8. For the PGS specimen, the maximum lateral force was 219 kN when the drift ratio was 2.2%. After longitudinal bars fractured, the lateral force decreased rapidly and the ultimate drift ratio was 3.6% as shown in Fig. 8(a). For the PUC specimen, when the drift ratio became to 2.8%, the lateral force reached to maximum value of 270 kN and the ultimate drift ratio was 5% with the core concrete crushed above the enlarged region of the column, like Fig. 8(b).

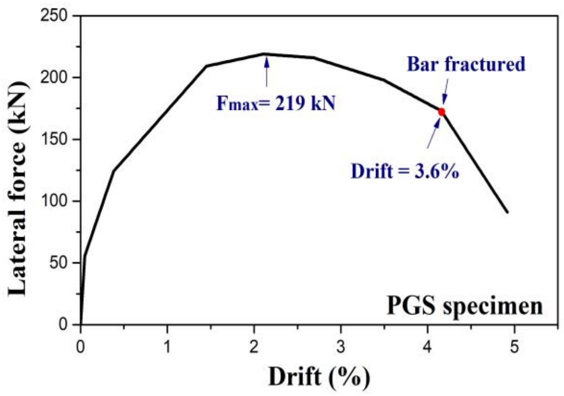

(a) PGS specimen

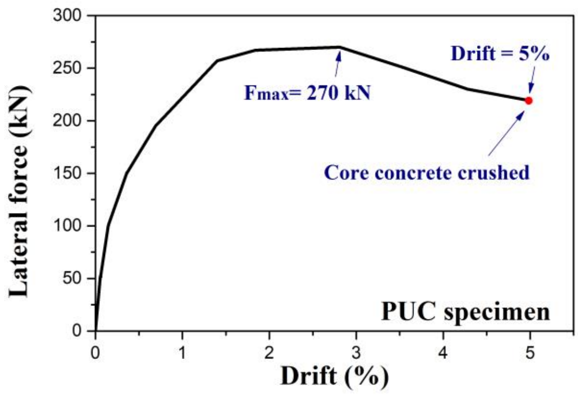

(b) PUC specimen

Fig. 8 – Average force-drift envelopes

4.3 Energy dissipation and residual drift

To evaluate energy dissipation capacity, the equivalent viscous damping at each drift ratio level of two specimens is shown in Fig.9. It can be seen that within the drift ratio of 1%, which means the specimen no damage or with slight damage, the equivalent viscous damping for both two specimens were approximately equaled to 5%. This regularity is commonly used in concrete structure analysis. Beyond 1% drift ratio level, the equivalent viscous damping of PGS specimen was growing faster, and the maximal equivalent viscous damping was 31.27%, as shown in Fig. 9(a). But for PUC specimen, the equivalent viscous damping increased steadily with the drift ratio and the maximum value was 24.20%, like Fig. 9(b).

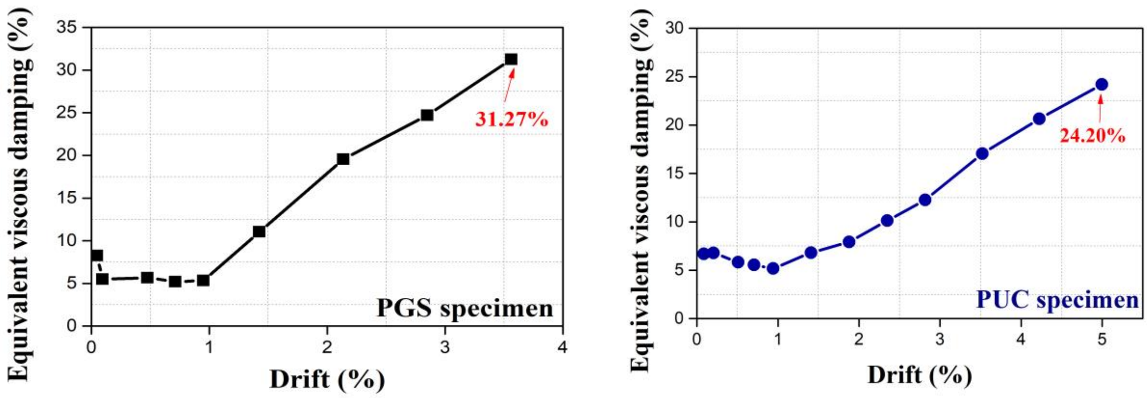

(a) PGS specimen (b) PUC specimen

Fig. 9 – Equivalent viscous damping of specimens

Fig.10 illustrates the residual drift ratio values at different levels for both specimens. In quasi-static tests, residual displacement is defined as the displacement of the specimen when the lateral loading force is zero, and the residual drift is the ratio of the residual displacement to loading height, which was 4210 mm for both two specimens. Before 1% drift ratio, little residual displacement was observed for both two specimens. With the increasment of lateral loading, the residual displacement emerged and the ultimate residual drift ratio of the two specimens are shown in Fig. 10(a) and Fig. 10(b) respectively.

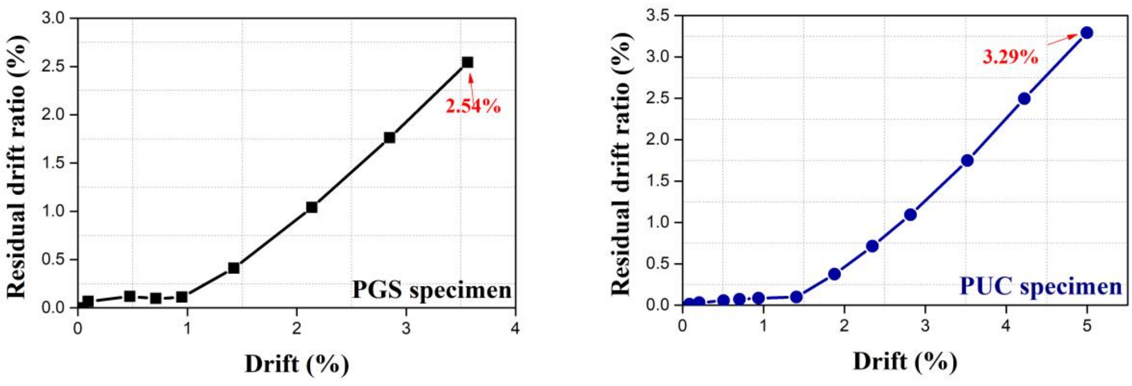

(a) PGS specimen (b) PUC specimen

Fig. 10 – Residual drift ratio of specimens

5. Conclusions

In this paper, two concrete precast bridge columns with different connection types were tested under cyclic loading to evaluate seismic response. One specimen used grouted sleeves connections and the other one used a new column-to-footing connection with UHPC. The following conclusions are the main findings of the experimental results:

(1) For the precast column with grouted sleeves connections, the grouted sleeves are inevitably stiffer than the longitudinal bars, so its presence affects the distribution of strains along the longitudinal bar and this led to the failure mode of the specimen was longitudinal bar fractured adjacent to the end of the sleeves.

(2) For the precast column connected with UHPC, the failure mode was the conventional core concrete crushed above the connection region and no damage such as cover concrete spalling or bar pullout was observed in the UHPC-filled connection.

(3) The quasi-static tests revealed that the failure modes of the two specimens with various connections were different, but no connection damage was observed for both specimens which means these kind of two connection types are appropriate precast connections for seismic regions.

6. Acknowledgements

This research is supported by the National Natural Science Foundation of China (Grant No. 51678434 and 51838010), which are gratefully acknowledged. The authors are also grateful to everyone who participated in these experimental projects for their selfless assistance.

7. References

[1] Shahawy M. (2003): Prefabricated Bridge Elements and Systems to limit traffic disruption during construction. *Technical Report*, Transportation Research Board, Washington, D.C., USA.

[2] Restrepo JI, Tobolski MJ, Matsumoto EE. (2011): Development of a precast bent cap system for seismic regions. *NCHRP Report 681*, Transportation Research Board, Washington, D.C., USA.

[3] Billington SL, Barnes RW, Breen JE (2001): Alternate substructure systems for standard highway bridges. *Journal of Bridge Engineering*, **6** (2), 87-94.

[4] Tazarv M, Saiidi MS (2014): Next generation of bridge columns for accelerated bridge construction in high seismic zones. *Report No. CCEER-14-06*, Center for Civil Engineering Earthquake Research, Department of Civil and Environmental Engineering, University of Nevada, Reno, Nevada.

[5] Ameli MJ, Brown DN, Parks JE, Pantelides CP (2016)：Seismic column-to-footing connections using grouted splice sleeves. *ACI Structural Journal*, **113** (5), 1021-1030.

[6] Graybeal BA (2006): Material property characterization of ultra-high performance concrete. *Report No: FHWA-HRT-06-103*, Fairfax, USA.

[7] Marsh ML, Wernli M, Garrett BE, Stanton JF, Eberhard MO, Weinert MD (2011): Application of accelerated bridge construction connections in moderate-to-high seismic regions. *NCHRP Report No. 698*, National Cooperative Highway Research Program, Washington, D.C., USA.

[8] Graybeal BA (2010): Behavior of Ultra-High Performance Concrete connections between precast bridge deck elements. *Proceedings of the 2010 Concrete Bridge Conference: Achieving Safe, Smart & Sustainable Bridges*, Phoenix, USA.

[9] Tazarv M , Saiidi MS (2015): UHPC-filled duct connections for accelerated bridge construction of RC columns in high seismic zones. *Engineering Structures*, **99**, 413-422.

[10] Ichikawa S, Matsuzaki H, Moustafa A, EIGawady MA (2016): Seismic-resistant bridge columns with ultrahigh-performance concrete segments. *Journal of Bridge Engineering*, **21** (9), 04016049.

